Digital Communication Using Chaotic-Pulse-Position Modulation

Nikolai F. Rulkov, Mikhail M. Sushchik, Lev S. Tsimring, and Alexander R. Volkovskii

Abstract—Utilization of chaotic signals for covert communications remains a very promising practical application. Multiple studies indicate that the major shortcoming of recently proposed chaos-based communication schemes is their susceptibility to noise and distortions in communication channels. In this paper, we review a new approach to communication with chaotic signals, which demonstrates good performance in the presence of channel distortions. This communication scheme is based upon chaotic signals in the form of pulse trains where intervals between the pulses are determined by chaotic dynamics of a pulse generator. The pulse train with chaotic inter-pulse intervals is used as a carrier. Binary information is modulated onto this carrier by the pulse position modulation method, such that each pulse is either left unchanged or delayed by a certain time, depending on whether "0" or "1" is transmitted. By synchronizing the receiver to the chaotic-pulse train we can anticipate the timing of pulses corresponding to "0" and "1" and thus can decode the transmitted information. Based on the results of theoretical and experimental studies we discuss the basic design principles for the chaotic-pulse generator, its synchronization, and the performance of the chaotic-pulse communication scheme in the presence of channel noise and filtering. We also discuss the possibilities of multiuser communication using CPPM and its advantages over standard communication techniques.

Index Terms—Chaos, nonlinear circuits, ultrawide band communication.

I. INTRODUCTION

EXPLOITING chaotic signals in communications has received significant attention in recent years [1]. The main premise in these studies is that broad-band signals generated by simple deterministic systems with chaotic dynamics can potentially replace pseudo-random carrier signals widely used in modern spread-spectrum communication systems (see for example, [2]). These pseudo-random sequences are generated by complex digital signal processors, and yet they are periodic due to the digital nature of the processor. In contrast, even a simple nonlinear circuit with very few off-the-shelf electronic components is capable of generating a very complex set of chaotic signals. The simplicity of chaos generators and the rich structure of chaotic signals are the two most attractive features of deterministic chaos that have caused a significant interest in possible utilization of chaos in communication.

Since the chaotic signal is nonperiodic, it cannot be stored in the receiver as a reference in order to achieve coherent detection of the transmitted signal. To overcome this problem, in some of the proposed communication schemes, the unmodulated chaotic waveform is transmitted along with the modulated signal (transmitted reference scheme) either using a separate channel or using time division [3]. Thus, a reliable detection can be achieved at the expense of at least 3 dB of the signal-to-noise ratio. In another approach, a chaotic reference is regenerated at the receiver using the phenomenon of chaotic synchronization [4]. This provides the key to recovery of information that is modulated onto a chaotic carrier [5]. A number of chaos-based covert communication schemes have been suggested [6], but most of them are very sensitive to distortions and noise [7], [8]. Phase distortions caused by filtering, are also very detrimental for the quality of chaos synchronization. This limits the use of filtering for noise reduction in chaos-based communications utilizing chaos synchronization. In [9], we proposed a way to avoid this difficulty by using chaotically timed pulse sequences rather than continuous chaotic waveforms. Each pulse has identical shape, but the time delay between them varies chaotically. Since the information about the state of the chaotic system is contained *entirely* in the timing between pulses, the distortions that affect the pulse shape will not significantly influence the ability of the chaotic-pulse generators to synchronize. Therefore, synchronizing chaotic-impulse generators can be utilized in communication schemes for realistic channels and at the same time allow the use of filters for noise reduction. The information can be encoded in the pulse train by alteration of time position of pulses with respect to chaotic carrier. This is the essence of the chaotic-pulse position modulation (CPPM) system [12]. When the receiver is synchronized with the transmitter, it can detect the delay between the expected and actual pulse arrival time, and thus decode the information. This proposed system belongs to the general class of ultrawide bandwidth wireless communication systems. These systems received significant attention recently [10] because they offer very promising alternative communication possibilities, especially in severe multipath environments or where they have to co-exist with a large number of other wireless systems. Chaotically varying spacing between narrow pulses enhances the spectral characteristics of the system by removing any periodicity from the transmitted signal. Because of the absence of characteristic frequencies, chaotically positioned pulses are difficult to observe and detect for an unauthorized user. Thus, one expects that transmission based on chaotic-pulse sequences can be designed to have a very low probability of intercept. A secure information transmission

based on chaotic-pulse trains with different method of information encoding, have been studied in [11].

The paper is organized as follows. Section II gives a detailed overview of the CPPM system. In Section III we describe our implementation of the CPPM system and present the results of the experimental performance analysis in communication through a model channel with noise, filtering, and attenuation. We also consider the limitations in its performance caused by parameter mismatch between transmitter and receiver. Theoretical and experimental studies of the CPPM performance in noisy environment are described in Section IV. In Section V we discuss implementation and characteristics of a low-power wireless CPPM communication system. Section VI describes a modification of the CPPM which improves the performance of CPPM in multiuser environment.

II. CPPM

In this section, we describe the CPPM. Consider a chaotic-pulse generator which produces chaotic-pulse signal

$$U(t) = \sum_{j=0}^{\infty} w(t - t_j) \tag{1}$$

where $w(t - t_j)$ represents the waveform of a pulse generated at time $t_j = t_0 + \sum_{n=0}^{j} T_n$, and T_n is the time interval between nth and $(n-1)$th pulses. We assume that the sequence of the time intervals, T_i, represents iterations of a chaotic process. For simplicity we will consider the case where chaos is produced by a one-dimensional map $T_n = F(T_{n-1})$, where $F(\ )$ is a nonlinear function. Some studies on such chaotic-pulse generators can be found in [9], [13].

The information is encoded within the chaotic-pulse signal by using additional delays in the generated inter-pulse intervals, T_n. As a result, the generated pulse sequence is given by a new map of the form

$$T_n = F(T_{n-1}) + d + mS_n \tag{2}$$

where S_n is the information-bearing signal. Here, we will consider only the case of binary information, and therefore, S_n equals to zero or one. The parameter m characterizes the amplitude of modulation. The parameter d is a constant time delay which is needed for practical implementation of our modulation and demodulation method. The role of this parameter will be specified later. In the design of the chaotic-pulse generator, the nonlinear function $F(\ )$, and parameters d and m are selected to guarantee chaotic behavior of the map.

The modulated chaotic-pulse signal $U(t) = \sum_{j=0}^{\infty} w(t - t_0 - \sum_{n=0}^{j} T_n)$, where T_n is generated by (2), is the transmitted signal. The duration of each pulse $w(t)$ in the pulse train is assumed to be much shorter than the minimal value of the inter-pulse intervals, T_n. To detect information at the receiver end, the decoder is triggered by the received pulses, $U(t)$. The consecutive time intervals T_{n-1} and T_n are measured and the information signal is recovered from the chaotic iterations T_n with the formula

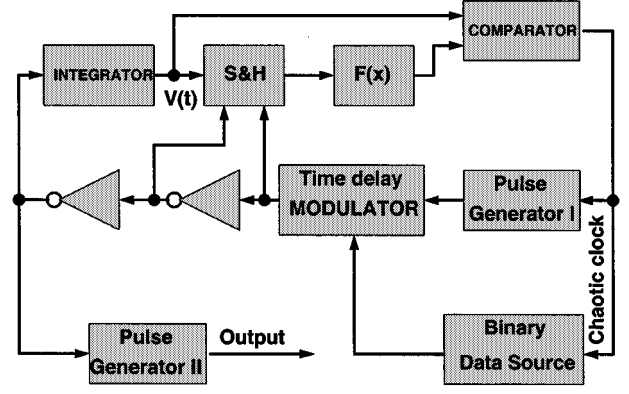$$S_n = (T_n - F(T_{n-1}) - d)/m. \tag{3}$$

Fig. 1.   Block diagram of the chaotic-pulse modulator.

If the nonlinear function, $F(\ )$, and parameters d and m in the receiver are the same as in the transmitter, then the encoded information, S_n, can be easily recovered. When the nonlinear functions are not matched with sufficient precision, a large decoding error results. Therefore, an unauthorized receiver who has no information on the dynamical system producing chaotic pulses in the transmitter, cannot determine whether a particular received pulse was delayed or not with respect to its original (chaotic) position, and thus whether S_n was "0" or "1".

Since the chaotic map of the decoder in the authorized receiver is matched to the map of the encoder in the corresponding transmitter, the time of the next arriving pulse can be predicted. In this case the input of the synchronized receiver can be blocked up to the moment of time when the next pulse is expected. The time intervals when the input to a particular receiver is blocked can be utilized by other users, thus providing a multiplexing strategy. Such selectivity based on the synchronization between the transmitter and the receiver can substantially improve the performance of the system by reducing the probability of false triggering of the decoder by channel noise.

In a noise-free environment, the arrival time of chaotic pulses can be easily registered by the threshold detector. However, in a noisy environment, the receiver can mistake a large noise fluctuation for a incoming pulse, and detect the wrong information bit. Furthermore, this false pulse can destroy chaotic synchronization, and thus prompt a sequence of errors until the receiver resynchronizes with the transmitter. In fact, one of the advantages of using chaotic-pulse generators is that the system reacquires synchronization automatically, without any specific "hand-shaking" protocol. The decoder only needs to detect two correct consecutive pulses in order to re-establish synchronization. We studied the bit-error performance in a noisy environment both theoretically and experimentally. The results of these studies are presented below in Section IV.

III. CPPM IMPLEMENTATION

A. CPPM Modulator

The implementation of the chaotic-pulse modulator used in our experiments is illustrated in Fig. 1. The integrator produces a linearly increasing voltage, $V(t) = \beta^{-1}(t - t_n)$, at its output. At the comparator this voltage is compared with the threshold voltage produced at the output of the nonlinear converter $F(x)$.

The threshold level $F(V_n)$ is formed by a nonlinear conversion of voltage $V_n = V(t_n)$ which was acquired and saved from the previous iteration using sample and hold (S&H) circuits. When voltage $V(t)$ reaches this threshold level, the comparator triggers the pulse generator I. It happens at the moment of time $t'_{n+1} = t_n + \beta F(V_n)$. The generated pulse (chaotic-clock signal) causes the data generator to update the transmitted information bit. Depending on the information bit transmitted, S_{n+1}, the delay modulator delays the pulse produced by the pulse generator by the time $d + mS_{n+1}$. Therefore, the delayed pulse is generated at the moment of time $t_{n+1} = t_n + \beta F(V_n) + d + mS_{n+1}$. Through the sample and hold circuit (S&H) this pulse first resets the threshold to the new iteration value of the chaotic map $V(t_{n+1}) \to F(V(t_{n+1}))$, and then resets the integrator output to zero, $V(t) = 0$. The dynamics of the threshold value is determined by the shape nonlinear function $F(\ )$. The spacing between the nth and $(n+1)$th pulses is proportional to the threshold value V_n, which is generated according to the map

$$T_{n+1} = \beta F(\beta^{-1} T_n) + d + mS_{n+1} \qquad (4)$$

where $T_n = t_{n-1} - t_n$, and S_n is the binary information signal. In the experimental setup the shape of the nonlinear function was built to have the following form:

$$F(x) \equiv \alpha f(x) = \begin{cases} \alpha x, & \text{if } x < 5V \\ \alpha(10V - x), & \text{if } x \geq 5V. \end{cases} \qquad (5)$$

The selection of the nonlinearity in the form of piecewise-linear function helps to ensure the robust regimes of chaos generation for rather broad ranges of parameters of the CPPM.

The position-modulated pulses, $w(t - t_j)$ are shaped in the pulse generator II. These pulses form the output signal $U(t) = \sum_{j=0}^{\infty} w(t - t_j)$, which is transmitted to the receiver.

B. CPPM Demodulator

When the demodulator is synchronized to the pulse position modulator, in order to decode a single bit of transmitted information the demodulator must simply determine whether or not a pulse from the transmitter was delayed relative to its anticipated position. If the ideal synchronization is established, but the signal is corrupted by noise, the optimal detection scheme operates as follows. Integrate the signal over the pulse duration inside the windows where pulses corresponding to "1" and "0" are expected to occur. The decision on whether "1" or "0" is received is made based upon whether the integral over "1"-window is larger or smaller than that over "0"-window. The performance of this scheme is known to be 3 dB worse than the BPSK system. Although in the case of perfect synchronization this detection scheme is ideal, according to our numerical simulations, its performance quickly degrades when synchronization errors due to the channel noise are taken into account. For this reason and for the sake of design simplicity we use a different approach to detection. The demodulator scheme is illustrated in Fig. 2.

In the receiver, the integrator, S&H circuits, and the nonlinear function block generating the threshold values are reset or triggered by the pulse received from the transmitter rather than by the pulse from the internal feedback loop. To be more
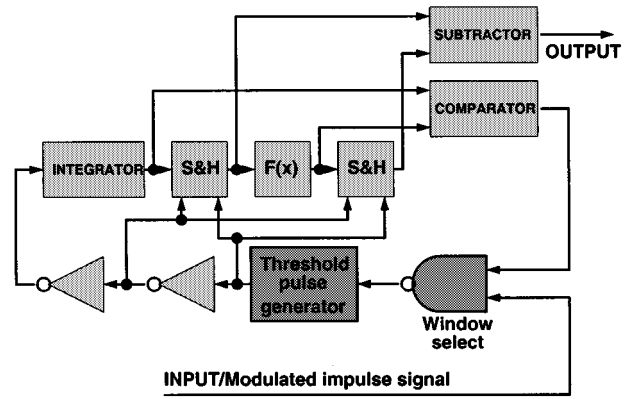

Fig. 2. Block diagram of the chaotic-pulse demodulator.

precise, they are triggered when the input signal $U(t)$ from the channel exceeds certain input threshold. The time difference between the anticipated location of the pulse without modulation, $t'_{n+1} = t_n + \beta F(V_n)$, and the actual arrival time t_{n+1} translates into the difference between the threshold value $F(V_n)$, generated by the nonlinear function and the voltage, $V(t_{n+1})$ at the integrator at the moment when the input signal $U(t)$ exceeds the input threshold. For each received pulse, the difference $V(t_{n+1}) - F(V_n)$ is computed and used for deciding whether or not the pulse was delayed. If this difference is less than the reference value $\beta(d + m/2)$, the detected data bit S_{n+1} is "0", otherwise it is "1".

Another important part of the receiver is the window select block. Once the receiver correctly observes two consecutive pulses, it can predict the earliest moment of time when it can receive the next pulse. This means that we can block the input to the demodulator circuit until shortly before such a moment. This is done by the window select block. In the experiment this circuit opens the receiver input at the time $t'_{n+1} = t_n + \beta F(V_n)$ by window control pulses generated by the comparator (see Fig. 2). The input stays open until the decoder is triggered by the first pulse received. Using such windowing greatly reduces the chance of the receiver being triggered by noise, interference, or pulses belonging to other users.

C. Parameters Mismatch Limitations

It is known that because the synchronization-based chaotic-communication schemes rely on the identity of synchronous chaotic oscillations, they are susceptible to negative effects of parameters mismatches. Here, we evaluate how precisely the parameters of our modulator and demodulator have to be tuned in order to ensure errorless communication over a distortion-free channel.

Since the information detection in our case is based on the measurements of time delays, it is important that the modulator and the demodulator can maintain synchronous time reference points. The reference point in the modulator is the front edge of the chaotic-clock pulse (CCP). The reference point in the demodulator is the front edge of the window control pulse. Ideally, if the parameters of the modulator and the demodulator were exactly the same and the systems were synchronized, then both reference points would be always at the times $t'_{n+1} = t_n + \beta F(V_n)$, and the received pulse would be delayed by the
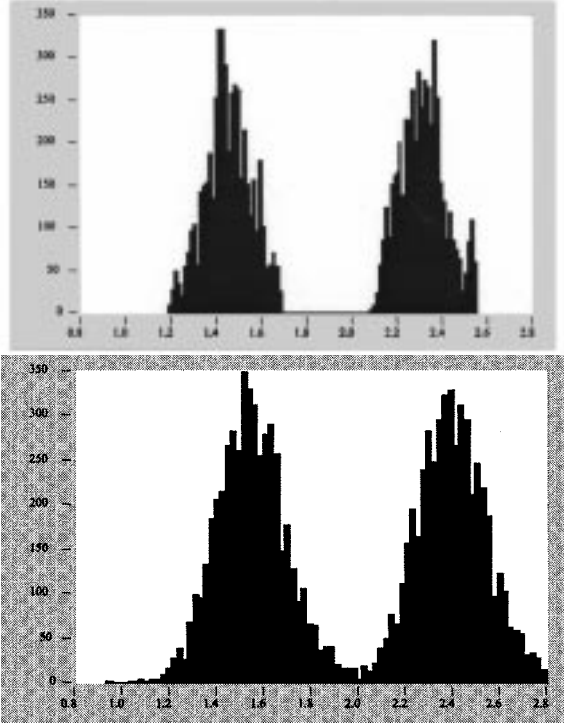
Fig. 3. Histograms of the fluctuations of the received pulse positions with respect to the receiver reference point: noise-free channel (top) and channel with WGN $E_b/N_o \sim 18$ dB (bottom).

time d for $S_{n+1} = 0$ and $d + m$ for $S_{n+1} = 1$. In this case, setting the bit separator at the delay $d + m/2$ would guarantee errorless detection in a noise-free environment.

In an analog implementation of a chaotic-pulse position modulator/demodulator system, the parameters of the circuits are never exactly the same. Therefore, the time positions $t_n'^{(M)}$ and $t_n'^{(D)}$ of the reference points in the modulator and the demodulator chaotically fluctuate with respect to each other. Due to these fluctuations, the position of the received pulse, $t_n = t_n'^{(M)} + d + S_n$, is shifted from the arrival time predicted in the demodulator, $t_n'^{(D)} + d + S_n$. The errors are caused by the following two factors. First, when the amplitude of fluctuations of the position shift is larger than $m/2$, some delays for "0"s and "1"s overlap and cannot be separated. Second, when the fluctuations are such that a pulse arrives before the demodulator opens the receiver input $(t_n < t_n'^{(D)})$, the demodulator skips the pulse, loses synchronization and cannot recover the information until it re-synchronizes. In our experimental setup the parameters $\beta_{M,D}$ were tuned to be as close as possible, and the nonlinear converters were built using 1% components. The fluctuations of the positions of the received pulses with respect to the window control pulse were studied experimentally by measuring time delay histograms. Fig. 3 presents typical histograms measured for the case of noise-free channel and for the channel with noise when $E_b/N_o \sim 18$ dB.

Assuming that systems were synchronized up to the $(n-1)$th pulse in the train, the difference between the reference time positions equals

$$\Delta_n \equiv t_n'^{(D)} - t_n'^{(M)}$$
$$= \beta_D F_D \left(\beta_D^{-1} T_{n-1} \right) - \beta_M F_M \left(\beta_M^{-1} T_{n-1} \right) \quad (6)$$
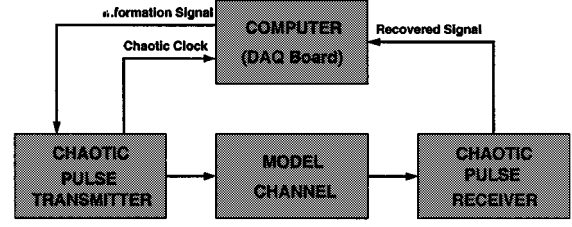

Fig. 4. Diagram of the experiment.

where indices D and M stand for demodulator and modulator, respectively. As was discussed, in order to achieve errorless detection, two conditions should be satisfied for all time intervals in the chaotic-pulse train produced by the modulator. These conditions are the synchronization condition, $\{\Delta_n\}_{\max} < d$, and the detection condition $\{|\Delta_n|\}_{\max} < m/2$. As an example we consider the simplest case where all parameters of the systems are the same except for the mismatch of the parameter α in the nonlinear function converter, see (5). Using (5) and (6) the expression for the separation time can be rewritten in the form

$$\Delta_n = (\alpha_D - \alpha_M)\beta f(\beta^{-1} T_{n-1}). \quad (7)$$

It is easy to show that the largest possible value of the nonlinearity output $f(\ )$, which can appear in the chaotic iterations of the map, equals to 5 V. Note that in the chaotic regime only positive values of $f(\ )$ are realized. Therefore, if conditions

$$\beta(\alpha_D - \alpha_M) < d/5V \quad \text{and} \quad 2\beta|\alpha_D - \alpha_M| < m/5V \quad (8)$$

are satisfied and there is no noise in the channel, then information can be recovered from the chaotic-pulse train without errors.

IV. CPPM PERFORMANCE EVALUATION

In our experiment (Fig. 4) we used a computer with a data acquisition board as the data source, triggered by the chaotic clock from the transmitter. We also used the computer to record the pulse displacement from the demodulator subtractor for every received pulse. This value was used to decode the information for the bit-error rate (BER) analysis. The model channel circuit consisted of WGN generator and a bandpass filter with the pass band 1 kHz–500 kHz. The pulse duration was 500 ns. The distance between the pulses varied chaotically between 12 μs and 25 μs. This chaotic-pulse train carried the information flow with the average bit rate ~ 60 kb/s. The amplitude of pulse position modulation, m, was 2 μs. The spectra of the transmitter output, noise and the signal at the receiver are shown in Fig. 5.

We characterize the performance of our system by studying the dependence of the BER on the ratio of energy per one transmitted bit to the spectral density of noise, E_b/N_0. This dependence is shown in Fig. 7, where it is compared to the performance of more traditional communication schemes, BPSK, PPM, and noncoherent FSK.

We can obtain a rough analytical estimate of the CPPM BER performance of our detection scheme in the case of rectangular pulse shape. In order to do so, let us consider a simplified model of our detection method. In the detector the signal that is a sum of the transmitted pulse signal and WGN is low-pass filtered and
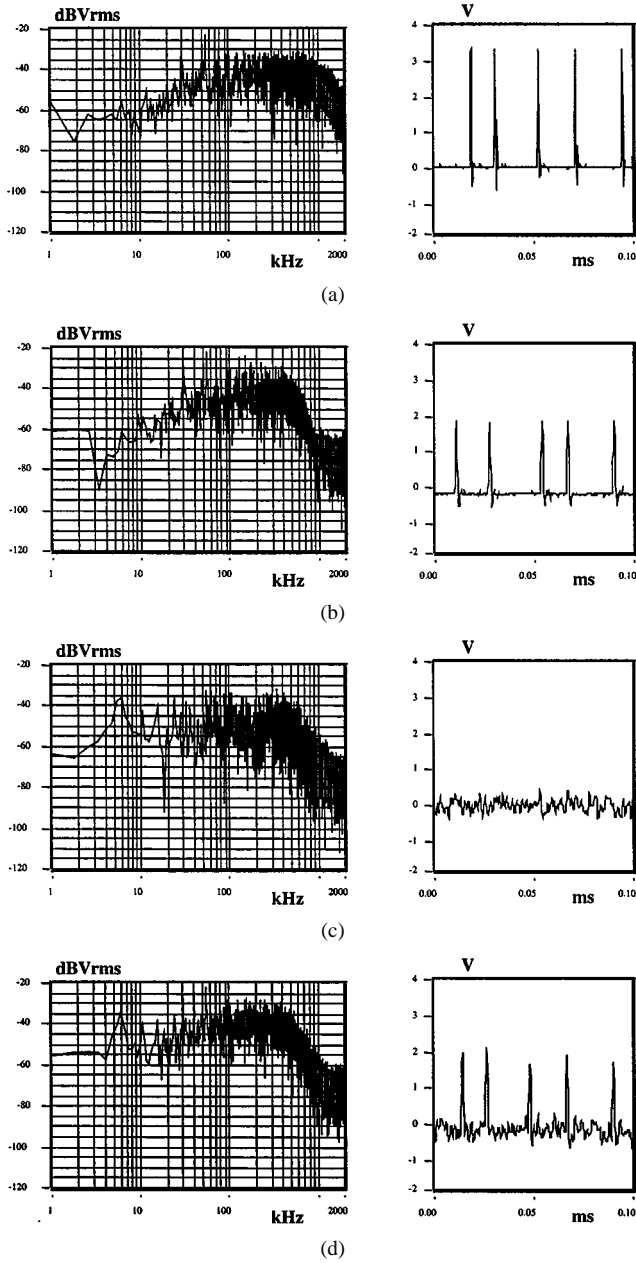
Fig. 5. Spectra and waveforms of signals in the channel: (a) Transmitter output. (b) Filtered transmitter output. (c) Filtered noise. (d) The received signal.
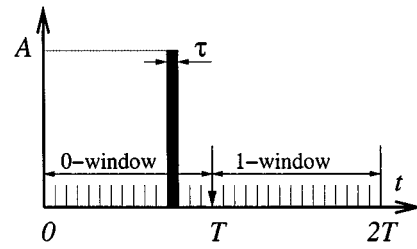

Fig. 6. Illustration of the detection scheme.

In our model detection scheme, the threshold element is set off when the output from one of the bins is larger than the threshold. If the threshold is crossed where a pulse corresponding to "0" is expected, a "0" is detected, otherwise a "1" is detected by default.

Let us introduce a few more notations. Let A be the pulse amplitude, H—the threshold value, and σ^2—the noise variance at the filter output.

Let us first evaluate the error probability when "1" is transmitted, $P_{0|1}$. This probability can be found from $P_{1|1}+P_{0|1} = 1$, where $P_{1|1}$, the probability to correctly detect "1" can be easily found. It is the probability that the filter output, y_i, from *any* bin in the "0" does not exceed the threshold. Using the statistical independence of the measurements for each window in the case of white noise, we can write

$$P_{1|1} = \prod_{i=1}^{T/\tau} p_i(y_i < H) = [p(y < H)]^{T/\tau}$$

$$= \left[\frac{1}{\sqrt{2\pi\sigma^2}} \int_{-\infty}^{H} \exp\left(-\frac{x^2}{2\sigma^2}\right) dx \right]^{T/\tau}$$

$$= \left[\frac{1}{2}\left(1 + \mathrm{erf}\left(\frac{H}{\sqrt{2\sigma^2}}\right)\right) \right]^{T/\tau}$$

$$= \left[\frac{1}{2}\left(1 + \mathrm{erf}\left(h\sqrt{\frac{E_b}{N_0}}\right)\right) \right]^{T/\tau}$$

Here, we introduced the relative threshold value, $h = H/A$, the energy per bit, $E_b = A^2\tau$, and the spectral power density of noise, $N_0 = 2\sigma^2\tau$.

The probability to detect "0" when "1" is transmitted is then

$$P_{0|1} = 1 - P_{1|1} = 1 - \left[\frac{1}{2}\left(1 + \mathrm{erf}\left(h\sqrt{\frac{E_b}{N_0}}\right)\right) \right]^{T/\tau}.$$

The error probability in the case when "0" is transmitted can be found similarly. The error occurs when the output from all bins in the "0" window remains lower than the threshold, in spite that the transmitted signal is nonzero within one of them

$$P_{1|0} = \left[\frac{1}{\sqrt{2\pi\sigma^2}} \int_{-\infty}^{H} \exp\left(-\frac{x^2}{2\sigma^2}\right) dx \right]^{T/\tau - 1}$$

$$\times \left[\frac{1}{\sqrt{2\pi\sigma^2}} \int_{-\infty}^{H} \exp\left(-\frac{(x-A)^2}{2\sigma^2}\right) dx \right]$$

is applied to a threshold element. Let us assume that the low pass filter can be approximated by the running average filter:

$$y(t) = \frac{1}{\tau} \int_{t-\tau}^{t} x(\xi)\, d\xi$$

Let the windows corresponding to "1" and "0" have the same duration, T, see Fig. 6. We shall assume that the receiver maintains synchronization at all times, so that every "0"-pulse is within the "0"-window, $0 < t \leq T$, and every "1"-pulse is within "1" window, $T < t \leq 2T$. Let us divide the interval where "0"-pulse is expected into bins of duration $1/f$, where f is the filter cut-off frequency. We shall assume that $f = 1/\tau, \tau$ being the pulse duration, and that when a pulse arrives, it is contained entirely within one bin. We shall sample the output $y(t)$ from the filter once at the end of every bin.
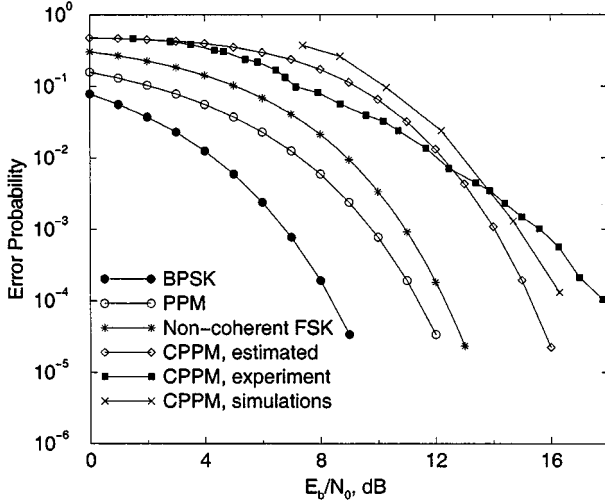
Fig. 7. Error probabilities of ideal BPSK, noncoherent FSK, and ideal PPM systems compared to the performance of the CPPM system.

$$= \left[\frac{1}{2} \left(1 + \mathrm{erf} \left(\frac{H}{\sqrt{2\sigma^2}} \right) \right) \right]^{T/\tau - 1}$$
$$\times \left[\frac{1}{2} \left(1 + \mathrm{erf} \left(\frac{H - A}{\sqrt{2\sigma^2}} \right) \right) \right]$$
$$= \left[\frac{1}{2} \left(1 + \mathrm{erf} \left(h\sqrt{\frac{E_b}{N_0}} \right) \right) \right]^{T/\tau - 1}$$
$$\times \left[\frac{1}{2} \mathrm{erfc} \left((1 - h)\sqrt{\frac{E_b}{N_0}} \right) \right].$$

The overall error probability is the combination of $P_{1|0}$ and $P_{0|1}$: $\mathrm{BER} = p_1 P_{0|1} + (1 - p_1) P_{1|0}$ where p_1 is the characteristic of the data stream which is the ratio of "1"s in it. In our experiment both p_1 and h were equal to $1/2$. In this case the expression for the BER can be written in a shorter form

$$\mathrm{BER} = \frac{1}{2} \left(1 - \mathrm{erf} \left(\frac{\sqrt{\epsilon}}{2} \right) \right.$$
$$\left. \times \left(\frac{1}{2} \left(1 + \mathrm{erf} \left(\frac{\sqrt{\epsilon}}{2} \right) \right) \right)^{T/\tau - 1} \right)$$

where $\epsilon = E_b / N_0$

Fig. 7 shows the BER performance of the CPPM as measured in the experiment, estimated analytically and computed in numerical simulations with $h = 0.5, p_1 = 0.5$ and $T/\tau = 10$. The difference of approximately 1 dB between the analytical and numerical curves can be largely attributed to burst errors arising from the loss of synchronization, which is not taken into account in our model. The slightly better than expected performance of the experimental system at high levels of noise can be explained by the observed in our setup significant deviations of the noise distribution from the Gaussian at high noise amplitudes. The quicker than expected degradation of performance at low levels of noise is primarily due to the small mismatch of the parameters in the transmitter and the receiver. Still, considering the crudeness of the analytical model and the experimental difficulties, all three plots agree reasonably well.
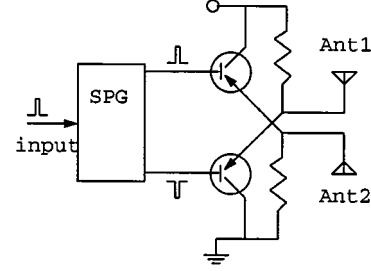

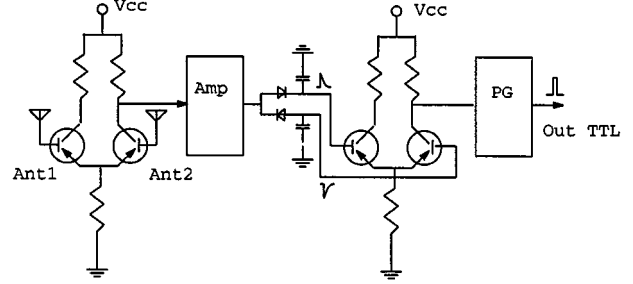Fig. 8. Block diagram of the ultrawide band transmitter used in the wireless CPPM communication system.

Fig. 9. Block diagram of the receiver used in the wireless CPPM system.

V. WIRELESS IMPLEMENTATION OF CPPM

We have implemented and tested a low-power prototype of the wireless digital communication link using the chaotic-pulse modulator and demodulator described above. The circuit diagrams of the transmitter and receiver units, which were added to the CPPM modulator and demodulator blocks to provide the wireless link, are shown in Figs. 8 and 9.

A. Transmitter and Receiver

The transmitter contains the generator of a pair of symmetric short pulses (SPG) and the symmetric exciter for the two-pole antenna, see Fig. 8. SPG is triggered by a TTL pulse (500 ns) from the output of the CPPM modulator (see Fig. 1) and generates a short pulse (20 ns measured at a half of the amplitude). This short pulse is applied to the symmetric exciter that has two outputs. The first output produces a high-voltage positive pulse. The second output produces a high-voltage negative pulse. These two outputs are applied to the corresponding poles of the antenna.

The block diagram of the receiver is presented in Fig. 9. The electromagnetic pulses received by the two-pole antenna (Ant1 and Ant2) are applied to the differential amplifier whose output is then amplified in the two-stage amplifier (Amp) and sent to the symmetric detector circuit. The output of the symmetric detector is then amplified by the second differential amplifier to generate enough voltage for triggering of pulse generator (PG) which produces the TTL pulse of the duration about 500 ns. The TTL pulse is then applied to the CPPM demodulator block shown in Fig. 2.

B. Spectral Characteristics of Transmitted CPPM Signals

We tested our prototype wireless CPPM system in indoor experiments with separation between transmitter and receiver of up to 15 m and were able to achieve a stable regime of error-free
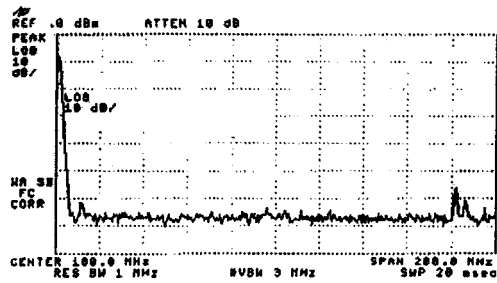
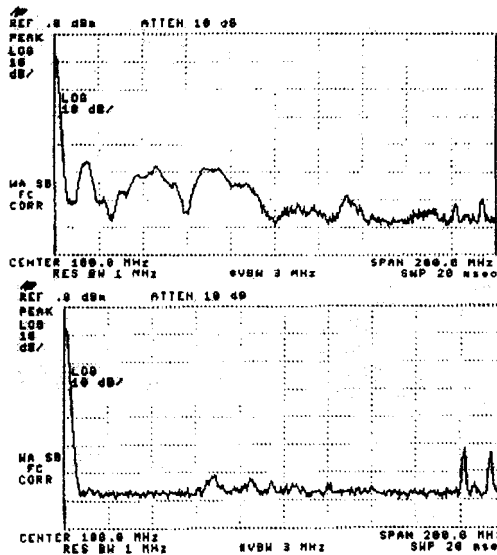Fig. 10.   PSD measured in the case when the CPPM transmitter turned off.

Fig. 11.   Spectra of the CPPM signal measured at the distance 1 m (top) and 10 m (bottom) from the CPPM transmitting antenna.
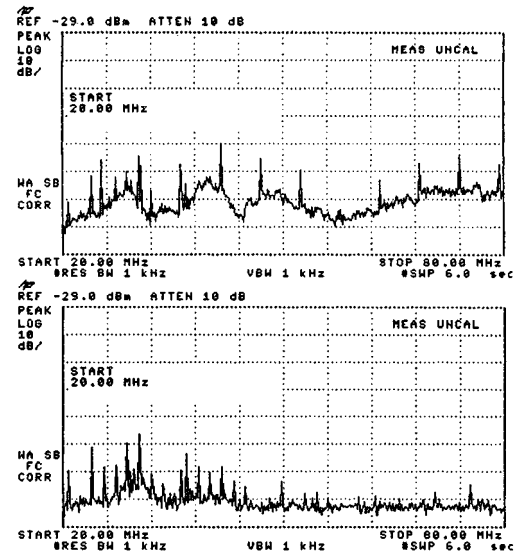

Fig. 12.   The spectrum of a transmission of a pulse train with pseudo-random pulse timing (top). The reference spectrum of the background (bottom). The start frequency is 20 MHz and the stop frequency is 80 MHz.
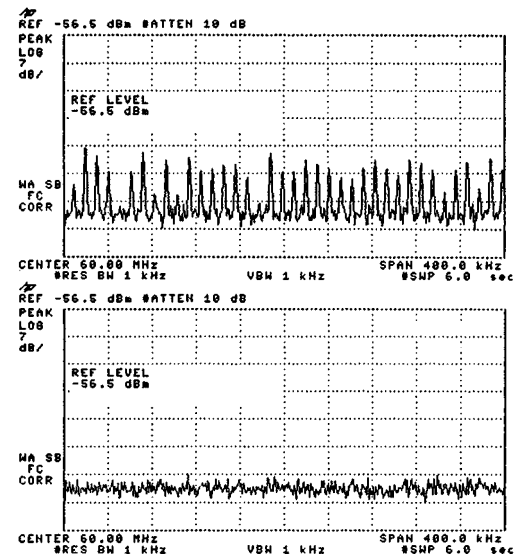

Fig. 13.   The spectrum of a transmission of a pulse train with pseudo-random pulse timing (the same as in the Fig. 12), but measured at a finer frequency resolution (top). A typical spectrum of a CPPM transmission measured with the same resolution (bottom).

communication. In these experiments we also studied spectral characteristics of the chaotic-pulse signal radiated by the wireless CPPM. Power-spectral density (PSD) was measured with HP 8590A Portable RF Spectrum Analyzer using two-pole receiving antenna. The results of the measurements are presented in Figs. 10 and 11. The PSD of the signal received by the RF spectrum analyzer, when CPPM transmitter is turned off, is shown in Fig. 10. The spectrum was measured in the range of frequencies from 1 MHz to 200 MHz with the video bandwidth filter of 3 MHz. The same measurements were done when the CPPM transmitter was turned on. The amplitude of the pulse measured across the poles of the transmitting antenna is about 130 V. Duration of the pulse is about 30 nsec. Fig. 11 presents measured PDS of the received RF signal at two distances from the transmitting antenna (1 and 10 m). As one can see, already at 10 m the signal PSD is at the level or below the background RF noise. This shows a potential for using CPPM systems in applications requiring low probability of detection.

C. CPPM and Low Probability of Detect

Here, we use the results of the experimental analysis of radiated pulse signals to illustrate the advantages of CPPM over more conventional communications schemes in the area of low probability of detection. The existing communication schemes rely on digitally generated pseudo-random sequences to eliminate from transmitted signals the features that allow an adver-

sary to detect and intercept the transmission. This approach has two intrinsic shortcomings.

First, the pseudorandom sequences eventually repeat, and second, the digital character of the generation algorithm introduces into the signal features associated with the corresponding quantization. These two points are illustrated in Fig. 12, where we show the spectrum of a pseudo-random pulse sequence transmitted by the same method as in the CPPM transmission. The transmitted signal consisted of a periodically repeated sequence of 128 pulses with the timing determined by the rising edges of a pseudo-random sequence of the length of 511 bits.

In Fig. 12 (top panel) one can clearly see the periodicity due to the quantization in the pseudo-random timing sequence, with the chip rate ~ 5.4 MHz. The peaks in Fig. 13 (top panel) are due

to the periodic repetition of the pseudo-random sequence, with the characteristic frequency ~ 10.5 kHz. Either of these features can be exploited in order to detect such transmission. For comparison, in the Fig. 13 (bottom panel) we see the spectrum of a chaotic-pulse train, with the same frequency resolution as in Fig. 13 (top panel). CPPM avoids both sources of periodicity present in the pseudo-random pulse train transmission, and, as expected, its spectrum does not show the corresponding peaks.

More complicated methods[1] used for detection of pseudo-random pulse transmissions can be applied in order to discover chaotic-pulse transmission. These methods however become much more efficient, if one can recover a time reference, which in the case of CPPM transmission is more difficult.

VI. MULTIUSER EXTENSION OF CPPM

Direct application of CPPM in a multiuser environment leads to a significant performance degradation. If multiple transmitters are operating at the same time, a receiver can capture pulses from other transmitters which would occasionally fit into the reception windows of the receiver, thus creating errors in the bit detection, and moreover, causing synchronization breakdowns. To reduce the probability of these events, we propose to send a fixed group of pulses instead of a single pulse. The structure of the pulse train should be unique for a given user, and the transmission time for the train as before is determined by the chaotic map. The detection of the pulse train arrival is achieved by the matched filter (correlation detector), thus providing selectivity and processing gain. The output of the correlator is then processed in the receiver in the same way as a single pulse is processed in the original scheme Fig. 2.

We tested this scheme in numerical simulations with up to 20 users. The pulse train patterns were chosen to minimize the maximum cross-correlation between different pulse trains. Chaotic intervals between the pulse trains were generated by the tent map with the slope 1.3. Then at the transmitter, the pulse train was produced either at time $T_n - \delta$ or $T_n + \delta$, depending on the value (0 or 1, respectively) of bit S_n being transmitted. Unlike the single-pulse CPPM, the detection scheme is based on the position of the maximum output of the correlator within a certain window with respect to the nominal (determined by the chaotic clock) position T_n. If the pulse train arrival time is closer to $T_n - \delta$ than to $T_n + \delta$, bit 0 is registered, and otherwise bit 1 is registered. We also employed adjustable window size depending on the magnitude of the output from the matched filter, so when the signal is weak (synchronization is lost), the window becomes large in order to re-establish synchronization. Fig. 14 shows the BER as a function of the number of users for 50-pulse trains. As was mentioned above, the performance of this system is degraded by occasional de-synchronization events. For comparison, a corresponding plot for ideally synchronized chaos oscillator at the receiver and transmitter, is shown. As can be seen,
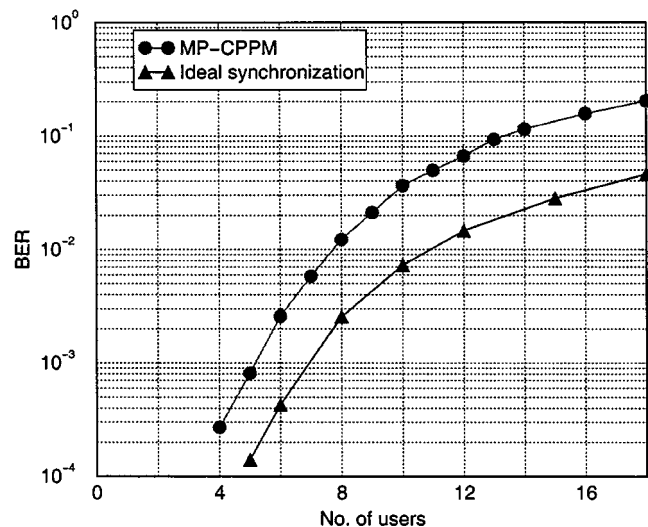

Fig. 14. BER as a function of the number of users in a multipulse CPPM scheme. Circles correspond to the MP-CPPM, and triangles to the case of line corresponds to the standard (periodic) PPM scheme.

the difference between these graphs is approximately 25% in terms of the number of users.

VII. CONCLUSION

Discussing chaos-based communication systems, one may notice a potential disadvantage common to all such schemes utilizing synchronization. Most traditional schemes are based on periodic signals and systems where the carrier is generated by a stable system. All such systems are characterized by zero Kolmogorov-Sinai entropy h_{KS} [15]: in these systems without any input the average rate of nonredundant information generation is zero. Chaotic systems have positive h_{KS} and continuously generate information. In the ideal environment, in order to perfectly synchronize two chaotic systems, one must transmit an amount of information per unit time that is equal to or larger than h_{KS} [15]. Although our detection method allows some tolerance in the synchronization precision, the need to transmit extra information to maintain the synchronization results in an additional shift of the actual CPPM performance curve relative to the case when ideal synchronization is assumed. Since the numerical and experimental curves in Fig. 7 pass rather close to the analytical curve that assumes synchronization, the degradation caused by nonzero Kolmogorov-Sinai entropy does not seem to be significant.

Although CPPM performs slightly worse than BPSK, noncoherent FSK and ideal PPM, we should emphasize that:1) this wide band system provides low probability of intercept and low probability of detection; 2) improves the privacy adding little circuit complexity; 3) to our knowledge, this system performs exceptionally well compared to most other chaos-based covert communication schemes [7]; 4) there exist a multiplexing strategy described above that can be used with CPPM (see also [16], [17]) (v) compared to other impulse systems, CPPM does not rely on a periodic clock, and thus can eliminate any trace of periodicity from the spectrum of the transmitted signal. All this makes CPPM attractive for development of chaos-based communications.

---

[1]We should point out that such simple and apparent scheme as observing a pulse sequence on an oscilloscope is not very efficient in noisy environment, with band-pass filtering due to antennas. Many (or all, if there is no transmission) pulses will appear due to noise.

ACKNOWLEDGMENT

REFERENCES

[1] *Special Issue in Noncoherent Chaotic Communications, IEEE Trans. Circuit. Syst. I*, vol. 47, pp. 1661–1764, Dec. 2000.

[2] G. Mazzini, G. Setti, and R. Rovatti, "Chaotic complex spreading sequences for asynchronous DS-CDMA— I: System modeling and results ," *IEEE Trans. Circuit. Syst. I*, vol. 44, no. 10, pp. 937–947, 1997.

[3] G. Kolumban, G. Kis, Z. Jákó, and M. P. Kennedy, "FM-DCSK: A robust modulation scheme for chaotic communications," *IEICE Trans. Fund.*, vol. E81-A, no. 9, pp. 1798–8002, 1998.

[4] L. M. Pecora and T. L. Carroll, "Synchronization in chaotic systems," *Phys. Rev. Lett.*, vol. 64, no. 8, pp. 821–824, 1990.

[5] C. W. Wu and L. O. Chua, "A simple way to synchronize chaotic systems with applications to secure communication systems," *Int. J. Bifurcation Chaos*, vol. 3, no. 6, pp. 1619–1627, 1993.

[6] M. Hasler, "Synchronization of chaotic systems and transmission of information," *Int. J. Bifurcation Chaos*, vol. 8, no. 4, pp. 647–659, 1998.

[7] C.-C. Chen and K. Yao, "Numerical evaluation of error probabilities of self-synchronized chaotic communications," *IEEE Commun. Lett.*, submitted for publication.

[8] N. F. Rulkov and L. S. Tsimring, "Synchronization methods for communications with chaos over band-limited channel," *Int. J. Circuit Theory Appl.*, vol. 27, no. 6, pp. 555–567, 1999.

[9] N. F. Rulkov and A. R. Volkovskii, "Synchronization of pulse-coupled chaotic oscillators," in *Proceedings of the Second Experimental Chaos Conference*. Singapore: World Scientific, 1993, pp. 106–115.

[10] M. Z. Win and R. A. Scholtz, "Impulse radio: How it works," *IEEE Commun. Lett.*, vol. 2, pp. 36–38, Feb. 1998.

[11] T. Yang and L. O. Chua, "Chaotic impulse radio: A novel chaotic secure communication system," *Int. J. Bifurcation Chaos*, vol. 10, no. 2, pp. 345–357, 2000.

[12] M. M. Sushchik *et al.*, "Chaotic pulse position modulation: A robust method of communicating with chaos," *IEEE Commun. Lett.*, vol. 4, pp. 128–130, 2000.

[13] P. A. Bernhardt, "Coupling of the relaxation and resonant elements in the autonomous chaotic relaxation oscillator (ACRO)," *Chaos*, vol. 2, no. 2, pp. 183–199, 1992.

[14] A. R. Volkovskii and N. F. Rul'kov, "Synchronous chaotic response of a nonlinear oscillator system as a principle for the detection of the information component of chaos," *Sov. Tech. Phys. Lett.*, vol. 19, no. 2, pp. 97–99, 1993.

[15] T. Stojanovski, Lj. Kocarev, and R. Harris, "Applications of symbolic dynamics in chaos synchronization," *IEEE Trans. Circuit. Syst. I*, vol. 44, pp. 1014–1017, Oct. 1997.

[16] H. Torikai, T. Saito, and W. Schwarz, "Multiplex communication scheme based on synchronization via multiplex pulse-trains," in *Proc. 1998 IEEE Int. Symp. Circuits and Systems*, New York, 1998, pp. 554–557.

[17] ——, "Synchronization via multiplex pulse-trains," *IEEE Trans. Circuit. Syst. I*, vol. 46, pp. 1072–1085, Sept. 1999.

Nikolai F. Rulkov received the M.S. and Ph.D. degrees, both in physics and mathematics, from the University of Nizhny Novgorod, Nizhny Novgorod, Russia, in 1983 and 1991, respectively.

In 1983, he joined the Radio Physics Department of the University of Nizhny Novgorod, where he worked as a Researcher until 1993. He has been with the Institute for Nonlinear Science, University of California, San Diego, from 1993 through the present. His research interests are in the areas of bifurcation theory, nonlinear phenomena, theory of synchronization, chaos and applications of chaotic oscillations in science and engineering.

Mikhail M. Sushchik was born in Nizhnii Novgorod, Russia, in 1970. He received the graduate degree and the Ph.D. degree in physics from the Polytechnical University of Nizhnii Novgorod, Nizhnii Novgorod, Russia, and the University of California, San Diego, in 1991, and 1996, respectively.

He is currently working as a Research Scientist at Therma-Wave, Inc., Fremont, CA. His research interests are mainly in the areas of nonlinear phenomena, synchronization, and theory and observation of chaotic oscillations.

Lev S. Tsimring was born in Saratov, Russia, in 1959. He received the graduate degree and the Ph.D. degree in physics and mathematics from the Gorky State University, Gorky, Russia and the P.P. Shirshov Institute of Oceanology, Moscow, Russia in 1980, and 1985, respectively.

Presently, he is a Research Scientist with the Institute for Nonlinear Science, at the University of California, San Diego. His research interests include nonlinear dynamics, chaotic synchronization, spatiotemporal chaos, pattern formation, and nonlinear signal processing.

Alexander R. Volkovskii was born in Nizhny Novgorod, Russia, in 1961. He received the M.S. degree from Lobachevskii State University, Nizhny Novgorod, Russia, in 1983, and the Ph.D. degree in radiophysics from Lobachevskii State University, Nizhny Novgorod, Russia, in 1994.

Since 1994, he has been with the Radiophysics Department, Lobachevskii State University, Nizhny Novgorod, Russia, as a Research Scientist and Assistant Professor. Currently, he is working as a Researcher at the Institute for Nonlinear Science, University of California, San Diego. His scientific interests include nonlinear dynamics and chaos in electronic circuits and computer simulations.